

## Preserving Symmetry and Degeneracy in the Localized Orbital Scaling Correction Approach

Neil Qiang Su<sup>§</sup>, Aaron Mahler<sup>§</sup>, and Weitao Yang\*



Cite This: *J. Phys. Chem. Lett.* 2020, 11, 1528–1535



Read Online

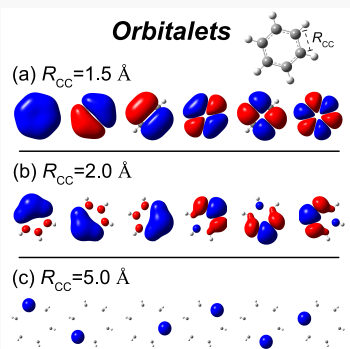
ACCESS |

Metrics & More

Article Recommendations

Supporting Information

**ABSTRACT:** Symmetry is a fundamental concept that plays a critical role in many chemical and physical phenomena and processes, which highlights the importance of theoretical methods to correctly handle symmetry. The recently developed localized orbital scaling correction (LOSC1) shows great improvement on the description of band gaps, photoemission spectra, and dissociation limits of cationic species. However, issues remain with LOSC1 in dealing with the symmetry and degeneracy of electronic states, which are also relevant to other methods using localization. In this work, we utilize a new method that deals with the physical-space and the energy-space localization on an equal footing. The resulting localized orbitals, i.e., orbitalets, are able to maintain more symmetry and the desired state degeneracy, which is important in calculating the electronic structure of both molecules and periodic bulk systems. Furthermore, the curvature matrix is redefined to improve potential energy curves for systems with stretched bonds, while retaining the correct dissociation limits. This new approach, termed LOSC2, includes only two fitting parameters. It maintains accuracy similar to that of LOSC1 over many properties, while overcoming LOSC1's deficiencies in symmetry and degeneracy. Our tests have shown that LOSC2 orbitalets possess the full- or subgroup of molecular symmetry if allowed, which preserves the state degeneracy. Tests on differently sized planar annulenes, odd-numbered allenes, and triphenylene again verify that LOSC2 is able to maintain the state degeneracy, while LOSC1 cannot. All the tests demonstrate the advantage of LOSC2 in the calculation of molecular systems and its potential for application to periodic bulk systems.



Symmetry plays an important role in physics, chemistry, and materials science.<sup>1–3</sup> As a fundamental concept, symmetry is intimately related to the electronic structure, which in turn defines the optical, electronic and chemical properties of the system under study. For example, molecular symmetry is very helpful in understanding state degeneracy, chirality, spectroscopy, reactivity, etc.<sup>1</sup> Similarly, translational symmetry is essential for the Bloch theorem, which makes periodic system calculations feasible.<sup>4</sup> Therefore, the symmetry of electronic structures is important and deserves prominent consideration in the development of new theoretical methods.

Kohn–Sham (KS) density functional theory (DFT)<sup>5–7</sup> has been widely used in the calculation of electronic structures of both molecular and bulk systems. Its success is made possible by the development of proper approximations to the unknown exchange–correlation (XC) energy. The past decades have seen remarkable progress in the development of density functional approximations (DFAs), such as local density approximations (LDAs),<sup>8–10</sup> generalized gradient approximations (GGAs),<sup>11–13</sup> meta-GGAs,<sup>14–18</sup> and hybrid GGAs,<sup>19–22</sup> which have become popular in practical applications because of their excellent performance-to-cost ratio as compared to wave function methods. Moreover, these types of approximations have the merit of no symmetry issues, and it is feasible to construct new functionals that satisfy many exact constraints.<sup>7,18</sup> Even so, there are still intrinsic errors in commonly

used DFAs, which can lead to spectacular failures in DFT calculations.<sup>23–33</sup> The delocalization error,<sup>24,25,28</sup> defined as the convex deviation from the Perdew–Parr–Levy–Balduz (PPLB) linearity condition for fractional charges,<sup>34–36</sup> is one of the dominant errors that lead to the problems in calculating ionization potentials (IPs), electron affinities (EAs), and reaction barriers. Another major systematic error is the static (or strong) correlation error, exhibited as the deviation from the exact conditions for fractional spins.<sup>26,35</sup> This work mainly focuses on the delocalization error.

In principle, the ever-increasing accuracy requirement in practical applications can be satisfied by developing better approximations. The development of doubly hybrid<sup>37–41</sup> and range-separated<sup>42–54</sup> functionals showed some promise in reducing delocalization error. Localized orbital scaling correction (LOSC) was developed in an effort to systematically address the delocalization error associated with commonly used DFAs in a size-consistent way.<sup>55</sup> To impose the PPLB condition on global and local regions in a dynamical way, orbitalets<sup>55</sup> are utilized. Orbitalets are a set of localized

Received: December 30, 2019

Accepted: January 31, 2020

Published: January 31, 2020

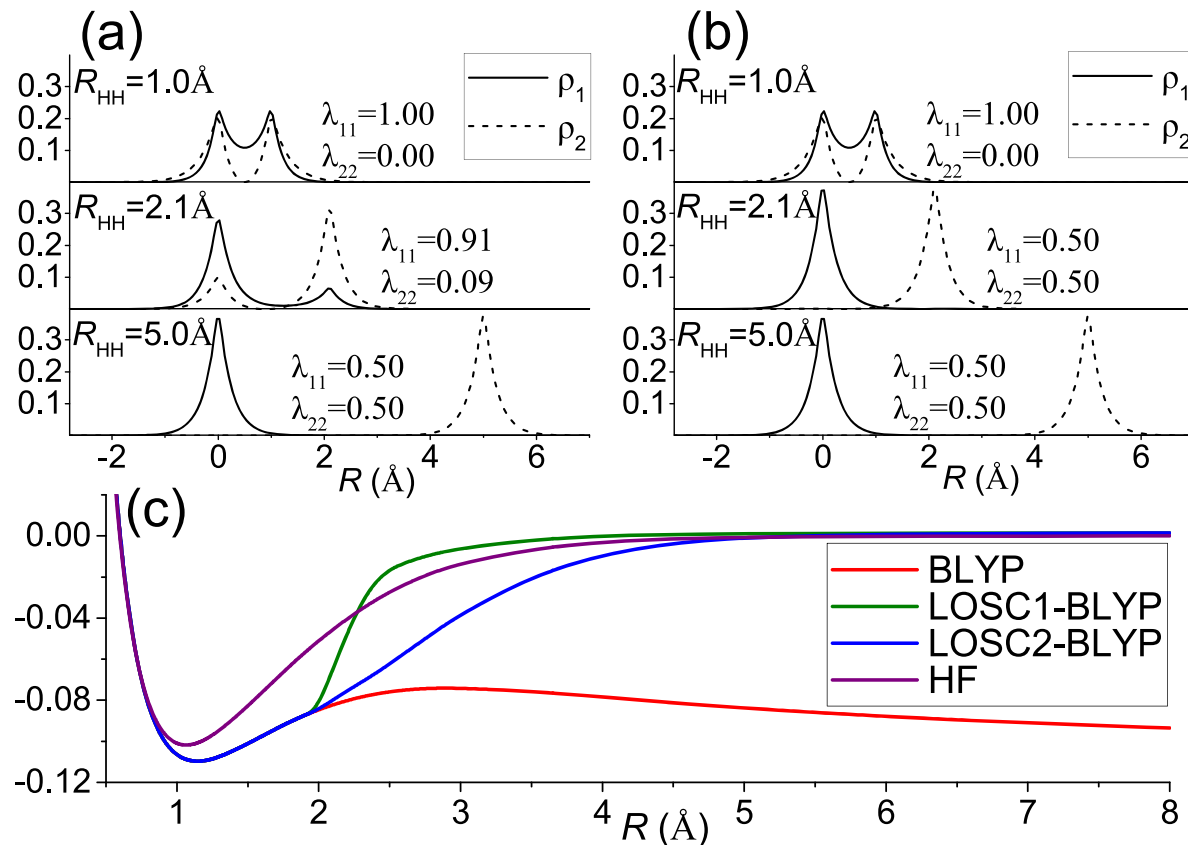


**Figure 1.** LO densities plotted along the bonding axis of  $\text{H}_2^+$  at the internuclear distances of  $R_{\text{HH}} = 1.0, 2.1$ , and  $5.0 \text{ \AA}$  for (a) LOSC1-BLYP and (b) LOSC2-BLYP. The two H atoms locate at  $x = 0.0$  and  $x = R_{\text{HH}}$ . (c) Potential energy curves for  $\text{H}_2^+$  dissociation. The energy of a doublet H atom is set to zero. Basis set cc-pVTZ<sup>56</sup> is used. All densities and energies are in atomic units.

orbitals (LOs) that are localized in both physical and energy spaces. For small systems at equilibrium with large orbital energy difference, orbitalets remain essentially canonical orbitals (COs); hence, the correction is imposed on entire systems. For stretched or larger systems with small band gaps, orbitalets become localized on each fragments, imposing the correction in local regions. These remarkable features give LOSC the ability to correct the total energy and orbital energies in a size-consistent manner. It greatly improves the descriptions of dissociation of cationic species, the band gaps of small-sized molecules and polymers, and photoemission spectra.<sup>55</sup>

While orbitalets capture fractional charge information that enables the effective correction to DFAs, we consider here the symmetry of orbitalets and its influence on the electronic structure of the LOSC approach, because orbitalets are localized for larger systems and localization has an impact on symmetry and degeneracy of the resulting generalized Kohn–Sham orbitals. As will be shown below, the symmetry of orbitalets determines the symmetry of the LOSC one-electron Hamiltonian, which thus influences the calculations of symmetry-related properties. For example, the symmetry of the Hamiltonian decides the state degeneracy (see section I of the Supporting Information) and is closely related to the Bloch theorem applied in the calculation of periodic systems (see section IV of the Supporting Information). To avoid confusion, the original LOSC is called LOSC1 in the following discussion. Here, orbitalets of LOSC1-BLYP for  $\text{H}_2^+$  at different H–H distances are plotted in Figure 1a. Being COs at equilibrium bond length, orbitalets transform through a

series of unsymmetric LOs during dissociation before they turn into two symmetric LOs at the dissociation limit. Thus, the orbital localization in LOSC1 can have an issue—it breaks the molecular symmetry and associated state degeneracy.

To address this challenge, we develop in the present work a modified objective function that treats the localizations of the physical and energy spaces on an equal footing. This leads to orbitalets that gain more symmetry, and the resulting method preserves state degeneracy.

The LOSC correction to total energy<sup>55</sup> is formulated as

$$\Delta E = \frac{1}{2} \sum_{pq} \lambda_{pq}^* (\delta_{pq} - \lambda_{pq}) \kappa[\rho_p, \rho_q] \quad (1)$$

where  $\delta_{pq}$  is the Kronecker delta function and  $\lambda$  and  $\kappa$  are occupation and curvature matrices, respectively. Because the off-diagonal elements of the  $\lambda$  matrix may be complex values in periodic system calculations using plane-wave basis sets, the LOSC correction to total energy has been slightly modified in eq 1 to guarantee that the correction is a real number. This is done by simply changing the first  $\lambda_{pq}$  to  $\lambda_{pq}^*$ . The occupation matrix is calculated via  $\lambda_{pq} = \langle \phi_p | \hat{\rho} | \phi_q \rangle$ ; thus,  $\lambda_{pq}^* = \lambda_{qp}$ . The curvature,  $\kappa[\rho_p, \rho_q]$ , takes the form of

$$\kappa[\rho_p, \rho_q] = (1 - d_{\text{X}}^{\text{HF}}) \left\{ \int d\mathbf{r}' \int d\mathbf{r} \frac{\rho_p(\mathbf{r}) \rho_q(\mathbf{r}')}{|\mathbf{r} - \mathbf{r}'|} - \frac{2\tau C_{\text{X}}}{3} \int d\mathbf{r} [\rho_p(\mathbf{r}) \rho_q(\mathbf{r})]^{2/3} d\mathbf{r} \right\} \quad (2)$$

where  $\tau = 1.2378$  and  $C_X = \frac{3}{4} \left(\frac{6}{\pi}\right)^{1/3}$ ;  $d_X^{\text{HF}}$  is the amount of HF exchange energy in the parent functional. Here, a set of LOs and their densities,  $\rho_p(\mathbf{r}) = |\phi_p(\mathbf{r})|^2$ , are needed to define the  $\lambda$  and  $\kappa$  matrices.

The desired LOs in LOSC are obtained by unitary transformation of both occupied and virtual COs, i.e.  $\phi_p(\mathbf{r}) = \sum_q U_{pq} \phi_q(\mathbf{r})$ . This is in contrast to other localization methods, such as the Foster–Boys localization,<sup>57</sup> which mixes only occupied or virtual COs. The transformation matrix  $U$  in LOSC1 is obtained by minimizing the following objective function:<sup>55</sup>

$$F = \sum_p \langle \phi_p(1) \phi_p(2) | (\mathbf{r}_1 - \mathbf{r}_2)^2 | \phi_p(1) \phi_p(2) \rangle + \sum_{pq} 2\omega_{pq} |\langle \phi_p | \phi_q \rangle|^2 \quad (3)$$

where the first term is for the physical-space localization, while the second term is the energy-space localization with an energy window. It should be noted that the penalty function,  $\omega_{pq}$  in the energy-space part, depends on the CO energy difference,  $|\epsilon_p - \epsilon_q|$ . Its purpose is to restrict the mixing of COs with large energy difference. This method of combining physical and energy spaces in the localization makes the orbitalets dynamical, which allows different and an appropriate amount of corrections to the delocalization error in common DFAs at different geometries. A fixed set of atomic orbitals such as those used in LDA+U cannot achieve this result.<sup>58–60</sup> The generalized transition state (GTS) method<sup>61</sup> and the work by Ma and Wang<sup>62</sup> make use of LOs from mixing of only occupied or virtual COs; thus, they cannot change the total energies for physical systems with integer number of electrons. Hence, these energy functionals are not size consistent and can correct only orbital energies (e.g., they cannot correctly describe the  $\text{H}_2^+$  dissociation); as pointed out previously, the necessity of changing the total energy of DFAs is critical to size-consistent nature of the correction.<sup>55</sup> The detailed comparison between LOSC with LDA+U and GTS has been provided in our previous publication.<sup>63</sup>

The LOSC correction for the one-electron Hamiltonian can be obtained by  $\delta\Delta E/\delta\rho$ . For simplicity, the contribution from the orbital relaxation is not taken into account, which actually works well.<sup>55</sup> Here, the correction to the Hamiltonian is formulated in a form similar to ref 64, that is

$$\Delta\hat{v} = \sum_{pq} |\phi_q\rangle \Lambda_{pq} \langle \phi_p| \quad (4)$$

where  $\Lambda_{pq} = \left(\frac{1}{2}\delta_{pq} - \lambda_{pq}\right)\kappa[\rho_p, \rho_q]$ , which depends not only on the density matrix but also on orbitalets. Ideally, the LOSC corrected Hamiltonian should have the system symmetry and thus

$$[\Delta\hat{v}, \hat{R}_n] = 0 \quad (5)$$

for the symmetry operators  $\hat{R}_n$  from the symmetry group of the system under study. Hence, the symmetry of the LOSC Hamiltonian is decided by orbitalets, and the satisfaction of eq 5 requires that the input orbitalets obey

$$\hat{R}_n\{\phi_p\} \equiv \{\phi_p\} \quad (6)$$

which means that for each LO with a symmetry operator acting on it, the resulting LO should be able to be reproduced by some LO from the original set of LOs (allowing for a prefactor difference); see the analysis in section V of the Supporting Information. Equation 6 poses a strict requirement on orbitalets. However, as shown in section I of the Supporting Information, the Hamiltonian with lower symmetry (subgroup of the complete symmetry) can also maintain the state degeneracy, which thus lowers the requirement for orbitalets. Note that normally COs cannot satisfy this requirement; thus, the global scaling correction (GSC)<sup>65</sup> cannot maintain the symmetry of the Hamiltonian.

The corrections to orbital energies are calculated via  $\Delta\epsilon_p = \langle \phi_p | \Delta\hat{v} | \phi_p \rangle$ .<sup>55</sup> The orbitalets obtained by minimizing eq 3 normally do not obey eq 6 for any subgroup of the molecular symmetry, resulting in the destruction of Hamiltonian symmetry and the associated state degeneracy. In perturbation theory, energy level splitting occurs when a perturbation of broken symmetry acts on the system under study. Thus, the destruction of degeneracy is easy to understand if the LOSC correction, eq 4, is treated as a perturbation to the Hamiltonian of the parent DFA.

To address the symmetry issue, here a different localization is utilized, with the objective function taking the form of

$$F = (1 - \gamma) \sum_p \Delta\mathbf{r}_p^2 + \gamma C \sum_p \Delta h_p^2 \quad (7)$$

where the usual definitions apply for  $\Delta\mathbf{r}_p^2 = \langle \mathbf{r}^2 \rangle_p - \langle \mathbf{r} \rangle_p^2$  and  $\Delta h_p^2 = \langle h^2 \rangle_p - \langle h \rangle_p^2$  ( $h$  being the one-electron Hamiltonian of the parent DFA), which are physical and energy spread functions for each LO. This objective function treats the physical space and the energy space in a similar manner, where the parameter  $\gamma$  allows for a continuous change between physical space localization and energy space localization. When  $\gamma = 0$ , the resulting orbitalets are maximally localized in physical space but delocalized in energy space; when  $\gamma = 1$ , then the orbitalets remain COs which are localized in energy space while being delocalized in physical space. A similar idea was suggested by Gygi et al.<sup>66–68</sup> to include the Hamiltonian in the objective function to obtain orbitals that are localized in physical space, while still being well confined in each local region of the eigenvalue spectrum. The key difference in our LOSC approach, eq 7, is that we always include both occupied and virtual COs in the localization, and let the CO energies and spatial delocalizations determine their mutual mixing. With this, the resulting fractional occupied LOs are able to capture fractional charge information on each local region for the LOSC correction.

The desired orbitalets in LOSC can be obtained by adjusting  $\gamma$  in eq 7. The constant  $C$  is for both conversion of units and matching magnitudes between the physical and energy spaces. As the energy space part is much smaller in value and is therefore multiplied by  $C = 10^3$  (in atomic units). The value of  $C$  does not affect any result, but it avoids the difficulty of parameter optimization when the desired  $\gamma$  is too close to the extreme value of 1. We obtain a value of  $\gamma = 0.707$ , which is optimized to obtain a balanced behavior on IPs and EAs of small-sized molecules and polymers. The algorithm of minimizing eq 7 through a series of  $2 \times 2$  rotations is provided in section II of the Supporting Information, which can be efficiently computed through an easily coded parallel implementation.

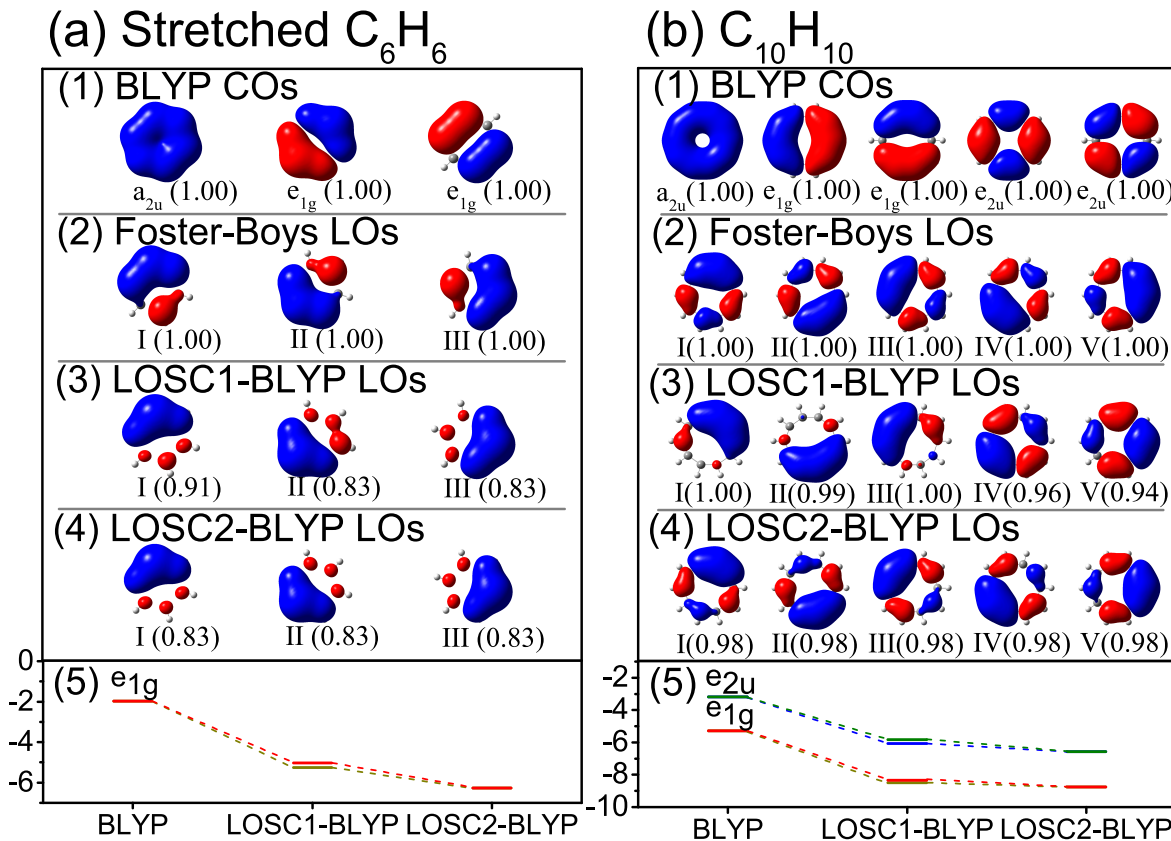


**Figure 2.** Comparison of LO symmetry and state degeneracy between LOSC1-BLYP and LOSC2-BLYP. (a) Stretched benzene ( $C_6H_6$  with  $R_{CC} = 2.0 \text{ \AA}$ ,  $D_{6h}$ ) and (b) planar [10]annulene ( $C_{10}H_{10}$  with  $R_{CC} = 1.5 \text{ \AA}$ ,  $D_{10h}$ ) tested with minimal basis set. These two systems are annulenes that satisfy Hückel's  $4n + 2$  rule for aromaticity.  $\pi$ -bond (1) delocalized COs of BLYP and LOs of (2) Foster-Boys, (3) LOSC1-BLYP and (4) LOSC2-BLYP are plotted. Here only occupied  $\pi$ -bonding COs and LOs with larger occupations are plotted; more results can be found in section VI of the Supporting Information. Each number in the parentheses is the occupation of each CO or LO, i.e., the expectation  $\langle \hat{\rho} \rangle$  of each orbital, which is proved in section V of the Supporting Information to be the same for symmetric LOs. (5) The degeneracy of a pair of states ( $e_{1g}$ ) for  $C_6H_6$  and two pairs of states ( $e_{1g}$  and  $e_{2u}$ ) for  $C_{10}H_{10}$  are checked. The y axis represents orbital energy in electronvolts. The dashed lines are just guides for the eye. LOSC1-BLYP breaks the degeneracy of  $e_{1g}$  ( $C_6H_6$ ),  $e_{1g}$  and  $e_{2u}$  ( $C_{10}H_{10}$ ) by around 0.2 eV, while LOSC2-BLYP guarantees the degeneracy of all the states. When cc-pVTZ is used, the energy of  $C_{10}H_{10}$  HOMOs ( $e_{2u}$ ) by BLYP is  $-5.4$  eV, which deviates greatly from  $-8.1$  eV by CCSD(T).<sup>71–73</sup> LOSC2-BLYP improves the energy to  $-8.5$  eV.

The orbitalets from the new localization for  $H_2^+$  dissociation can be found in Figure 1b. At both equilibrium bond length and the dissociation limit, the orbitalets are the same as those from the localization of eq 3. The main difference is that orbitalets are now symmetric in the middle range of bond lengths, which indicates that the new objective function of eq 7 is able to maintain the symmetry for orbitalets. Although the symmetry of new orbitalets cannot be strictly derived in general, in the following tests, it will be shown that the new orbitalets can maintain more symmetry.

Moreover, as shown in Figure 1c, the energy dissociation curve of LOSC1-BLYP shows a sharp shift at the point where the COs begin to mix with each other into LOs. For the energy correction of eq 1, the diagonal terms are positive, which restores the PPLB condition on each local region; while the off-diagonal terms are negative, which are needed for retrieving the correct asymptotic behavior when two fragments are far apart.<sup>55</sup> However, the off-diagonal elements of the  $\kappa$  matrix that are associated with two LOs on different fragments decay too fast as the fragments move away from each other, and thereby the negative terms in eq 1 decay rapidly, resulting in a sharp upward shift in the dissociation curve (see Figure 1c). To fix this, the curvature matrix is now revised as

$$\tilde{\kappa}[\rho_p, \rho_q] = \text{erf}(\zeta S_{pq}) \sqrt{|\kappa[\rho_p, \rho_p] \kappa[\rho_q, \rho_q]|} + \text{erfc}(\zeta S_{pq}) \kappa[\rho_p, \rho_q] \quad (8)$$

where  $\kappa[\rho_p, \rho_q]$  is from eq 2 and  $S_{pq}$  is calculated via  $\int \sqrt{\rho_p(\mathbf{r}) \rho_q(\mathbf{r})} d\mathbf{r}$ . This new definition changes the off-diagonal elements while keeping the diagonal elements unchanged, i.e.  $\tilde{\kappa}[\rho_p, \rho_p] = \kappa[\rho_p, \rho_p]$ , which is essential to guarantee the adherence to the PPLB condition on local regions. For an off-diagonal element associated with two LOs on different fragments,  $\sqrt{|\kappa[\rho_p, \rho_p] \kappa[\rho_q, \rho_q]|}$  reduces the decay rate of  $\tilde{\kappa}[\rho_p, \rho_q]$ ; moreover, because of the error functions in eq 8,  $\tilde{\kappa}[\rho_p, \rho_q]$  would reduce to  $\kappa[\rho_p, \rho_q]$  at the dissociation limit, ensuring the correct asymptotic behavior. The parameter  $\zeta$ , which is set at 8.0, allows for adjusting the rate at which the error functions change; it is optimized for generating a smooth dissociation curve for  $H_2^+$  (see Figure 1c).

This concludes the construction of the new version of LOSC, denoted as LOSC2. It mainly has three improvements: (i) The correction to total energy has been modified to guarantee that the correction of eq 1 is a real number and the corresponding correction to the Hamiltonian eq 4 is Hermitian

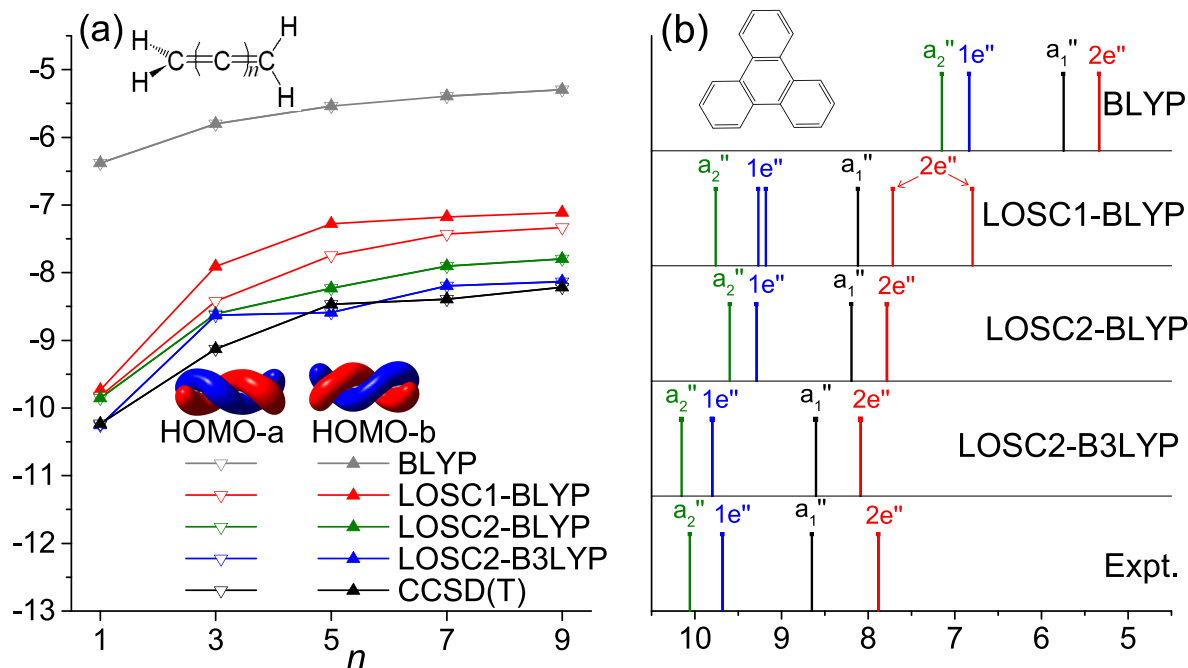


**Figure 3.** Comparison of the energy level and state degeneracy among BLYP, LOSC1-BLYP, LOSC2-BLYP, and LOSC2-B3LYP. (a) HOMOs of odd-numbered alenes are tested. Odd-numbered alenes have doubly degenerate HOMOs, which are helical and of symmetry  $e$ ; hence, they are achiral. Misprediction of the degeneracy of the two HOMOs would lead to misjudgment of the molecular chirality. The  $y$  axis represents orbital energy in electronvolts. The CCSD(T) results are used as reference. (b) Vertical ionization potentials of triphenylene ( $D_{3h}$ ) are tested, where  $1e''$  and  $2e''$  are two pairs of doubly degenerate states. The  $x$  axis represents IPs in electronvolts. Experimental results are from ref 74. All geometries are optimized by B3LYP.

for complex-valued wave functions. (ii) The objective function eq 7 that treats both physical and energy space localizations on an equal footing has been utilized so that the orbitalets keep more symmetry, which is very important for the calculation of the electronic structure of both molecular and bulk systems. (iii) The curvature matrix is redefined in eq 8 to generate smooth dissociation curves. LOSC2 has been tested on a variety of properties. The tests include reaction barrier heights (on HTBH38/08 and NHTBH38/08<sup>69</sup>), thermochemistry (on G2-97<sup>70</sup>), and IPs and EAs of small-sized molecules (on G2-97<sup>70</sup>) and polymers (polyacenes and polyacetylenes) (see section VI of the Supporting Information). All the tests show that LOSC2 with only two fitting parameters can achieve accuracy similar to that of LOSC1. LOSC2 greatly improves the performance of commonly used DFAs on IPs and EAs, while the test results of reaction barriers and thermochemistry remain unchanged. The problem of commonly used DFAs in predicting reaction barriers is mainly due to the delocalization error in approximate functionals.<sup>24</sup> However, LOSC2 cannot generate fractionally occupied LOs for small systems with big highest occupied molecular orbital–lowest unoccupied molecular orbital (HOMO–LUMO) gaps; thus, it provides no correction for reaction barriers of the systems tested here. Besides, LOSC2 is specially developed for reducing the delocalization error in approximate functionals; the combination with the fractional-spin correction is necessary to have better performance for strongly correlated systems.<sup>63</sup> It should be noted that the development here emphasizes the form of LOSC2 functional and its physical basis, rather than the fitting of the two parameters in the functional. The meaning of these two parameters has been clarified above.

In addition to the case of  $\text{H}_2^+$  dissociation, here show more examples about symmetry and degeneracy, where LOSC2 outperforms LOSC1. First, the LO symmetry and state degeneracy of planar annulenes ( $\text{C}_{4n+2}\text{H}_{4n+2}$ ) that satisfy Hückel's  $4n + 2$  rule for aromaticity are checked (see Figure 2 and section VI of the Supporting Information). For  $\text{C}_6\text{H}_6$  ( $D_{6h}$ ) at around equilibrium geometry, both LOSC1-BLYP and LOSC2-BLYP rarely mix the six  $\pi$ -bond COs (three occupied and three virtual) with each other because of their small size in physical space and large difference in energy space. As the C–C bonds stretch, the  $\pi$ -bond COs become larger in physical space and their energy difference shrinks, so that they will mix with each other into fractionally occupied LOs. Figure 2a shows the three LOs with larger occupations at  $R_{\text{CC}} = 2.0$  Å. LOSC1-BLYP cannot generate symmetric LOs; thus, it breaks the degeneracy of HOMOs, i.e.  $e_{1g}$  states, by around 0.2 eV. For LOSC2-BLYP, the LOs possess the symmetry of  $D_{3h}$ ; that is, LOs obey eq 6 for any symmetry operator from  $D_{3h}$ . Hence, the LOSC2 Hamiltonian is of  $D_{3h}$  symmetry too. As shown in section I of the Supporting Information, this lower symmetry of Hamiltonian does preserve the degeneracy of states in  $\text{C}_6\text{H}_6$ , so that LOSC2-BLYP is able to maintain the state degeneracy. In contrast to  $\text{C}_6\text{H}_6$ , the  $\pi$ -bond COs of  $\text{C}_{10}\text{H}_{10}$  at around equilibrium geometry already have a large spatial variance; thus, the COs tend to mix with each other into LOs. Similarly, LOSC2-BLYP can provide symmetric LOs and maintain state degeneracy for  $\text{C}_{10}\text{H}_{10}$ , while LOSC1-BLYP cannot (see Figure 2b). The examples of differently sized annulenes shown here are useful for a preliminary understanding of the calculation of bulk systems. In bulk systems, COs become more delocalized over physical space, implying they will inevitably mix with each

other into LOs. Hence, LOSC2 is particularly useful because it is able to provide symmetric LOs. For comparison, LOs of Foster–Boys are also plotted, the LOs also show lower symmetries, which are of  $C_{3h}$  symmetry for  $C_6H_6$  and of  $C_{5h}$  symmetry for  $C_{10}H_{10}$ .

It has been found that odd-numbered allenes possess doubly degenerate HOMOs which are composed of the right- and left-handed helices orientated at  $90^\circ$  from each other; hence, they are achiral.<sup>75</sup> Misprediction of the degeneracy of the two HOMOs would lead to misjudgment of the molecular chirality. As shown in Figure 3a, BLYP has the correct state degeneracy, but it overestimates HOMO energies. LOSC1-BLYP improves the orbital energies; however, it splits the degenerate HOMOs by around 0.5 eV. In contrast, LOSC2-BLYP improves the orbital energies while preserving the state degeneracy. Another example is vertical IPs of triphenylene (see Figure 3b).  $1e''$  and  $2e''$  are two pairs of doubly degenerate states. Both LOSC1-BLYP and LOSC2-BLYP improve the prediction of IP values. However, LOSC1-BLYP breaks the degeneracy of both  $1e''$  and  $2e''$ , while LOSC2-BLYP is able to maintain the degeneracy. For comparison, Figure 3 provides also the results of LOSC2-B3LYP, which further improves the orbital energies of LOSC2-BLYP.

In summary, the excellent performance of the LOSC approach reflects the capability of orbitalets for constructing functionals, making it critical to further discuss the orbitalet symmetry and its effect on state degeneracy. To address the issue of broken symmetry and degeneracy in LOSC1, the new localization utilized here allows orbitalets to preserve more symmetry and maintain the desired degeneracy in LOSC2, which is important for electronic structure calculations. Furthermore, LOSC2 outperforms LOSC1 in generating smooth dissociation curves, while maintaining the similar accuracy as LOSC1 over many properties. All the tests here demonstrate the advantage of LOSC2 in the calculation of molecular systems and its potential in the application of periodic bulk systems.

## ■ ASSOCIATED CONTENT

### Supporting Information

The Supporting Information is available free of charge at <https://pubs.acs.org/doi/10.1021/acs.jpcllett.9b03888>.

More mathematical derivations and calculation results (PDF)

## ■ AUTHOR INFORMATION

### Corresponding Author

Weitao Yang – Department of Chemistry, Duke University, Durham, North Carolina 27708, United States; Key Laboratory of Theoretical Chemistry of Environment, School of Chemistry and Environment, South China Normal University, Guangzhou 510006, China;  [orcid.org/0000-0001-5576-2828](https://orcid.org/0000-0001-5576-2828); Email: [weitao.yang@duke.edu](mailto:weitao.yang@duke.edu)

### Authors

Neil Qiang Su – Department of Chemistry, Duke University, Durham, North Carolina 27708, United States;  [orcid.org/0000-0001-7133-2502](https://orcid.org/0000-0001-7133-2502)

Aaron Mahler – Department of Physics, Duke University, Durham, North Carolina 27708, United States

Complete contact information is available at: <https://pubs.acs.org/10.1021/acs.jpcllett.9b03888>

### Author Contributions

<sup>§</sup>N.Q.S. and A.M. contributed equally to this work

### Notes

The authors declare no competing financial interest.

## ■ ACKNOWLEDGMENTS

The authors acknowledge support from the Center for Complex Materials from First-Principles (Temple University Subawd 262850-02), an Energy Frontier Research Center funded by the U.S. Department of Energy, Office of Science, Basic Energy Sciences (N.Q.S.); the National Science Foundation (Grant No. CHE-1900338) (W.Y.); and the Molecular Sciences Software Institute Phase-II Software Fellowship (A.M.).

## ■ REFERENCES

- (1) Cotton, F. *Chemical Applications of Group Theory*; Wiley, 1990.
- (2) Wherrett, B. *Group Theory for Atoms, Molecules, and Solids*; Prentice-Hall International, 1986.
- (3) Lax, M. *Symmetry Principles in Solid State and Molecular Physics*; Wiley, 1974.
- (4) Ashcroft, N.; Mermin, N. *Solid State Physics*, HRW international ed.; Holt, Rinehart and Winston, 1976.
- (5) Kohn, W.; Sham, L. J. Self-Consistent Equations Including Exchange and Correlation Effects. *Phys. Rev.* **1965**, *140*, A1133–A1138.
- (6) Hohenberg, P.; Kohn, W. Inhomogeneous Electron Gas. *Phys. Rev.* **1964**, *136*, B864–B871.
- (7) Parr, R. G.; Yang, W. *Density-Functional Theory of Atoms and Molecules*; Oxford University Press: New York, 1989.
- (8) Slater, J. C. *Quantum Theory of Molecules and Solids*; McGrawHill: New York, 1974; Vol. 14.
- (9) Vosko, S. H.; Wilk, L.; Nusair, M. Accurate Spin-Dependent Electron Liquid Correlation Energies for Local Spin Density Calculations: a Critical Analysis. *Can. J. Phys.* **1980**, *58*, 1200–1211.
- (10) Perdew, J. P.; Wang, Y. Accurate and Simple Analytic Representation of the Electron-Gas Correlation Energy. *Phys. Rev. B: Condens. Matter Mater. Phys.* **1992**, *45*, 13244–13249.
- (11) Becke, A. D. Density-Functional Exchange-Energy Approximation with Correct Asymptotic-Behavior. *Phys. Rev. A: At., Mol., Opt. Phys.* **1988**, *38*, 3098–3100.
- (12) Lee, C.; Yang, W.; Parr, R. G. Development of the Colle-Salvetti Correlation-Energy Formula into a Functional of the Electron Density. *Phys. Rev. B: Condens. Matter Mater. Phys.* **1988**, *37*, 785.
- (13) Perdew, J. P.; Burke, K.; Ernzerhof, M. Generalized Gradient Approximation Made Simple. *Phys. Rev. Lett.* **1996**, *77*, 3865–3868.
- (14) Van Voorhis, T.; Scuseria, G. E. A Novel Form for the Exchange-Correlation Energy Functional. *J. Chem. Phys.* **1998**, *109*, 400–410.
- (15) Boese, A. D.; Handy, N. C. New Exchange-Correlation Density Functionals: The Role of the Kinetic-Energy Density. *J. Chem. Phys.* **2002**, *116*, 9559–9569.
- (16) Tao, J.; Perdew, J. P.; Staroverov, V. N.; Scuseria, G. E. Climbing the Density Functional Ladder: Nonempirical Meta-Generalized Gradient Approximation Designed for Molecules and Solids. *Phys. Rev. Lett.* **2003**, *91*, 146401.
- (17) Zhao, Y.; Truhlar, D. G. A New Local Density Functional for Main-Group Thermochemistry, Transition Metal Bonding, Thermochemical Kinetics, and Noncovalent Interactions. *J. Chem. Phys.* **2006**, *125*, 194101.
- (18) Sun, J.; Ruzsinszky, A.; Perdew, J. P. Strongly Constrained and Appropriately Normed Semilocal Density Functional. *Phys. Rev. Lett.* **2015**, *115*, 036402.
- (19) Becke, A. D. Density-Functional Thermochemistry. III. The Role of Exact Exchange. *J. Chem. Phys.* **1993**, *98*, 5648–5652.
- (20) Stephens, P. J.; Devlin, F. J.; Chabalowski, C. F.; Frisch, M. J. Ab Initio Calculation of Vibrational Absorption and Circular

Dichroism Spectra Using Density Functional Force Fields. *J. Phys. Chem.* **1994**, *98*, 11623–11627.

(21) Ernzerhof, M.; Scuseria, G. E. Assessment of the Perdew-Burke-Ernzerhof Exchange-Correlation Functional. *J. Chem. Phys.* **1999**, *110*, 5029–5036.

(22) Adamo, C.; Barone, V. Toward Reliable Density Functional Methods Without Adjustable Parameters: The PBE0 Model. *J. Chem. Phys.* **1999**, *110*, 6158–6170.

(23) Mori-Sánchez, P.; Cohen, A. J.; Yang, W. Many-Electron Self-Interaction Error in Approximate Density Functionals. *J. Chem. Phys.* **2006**, *125*, 201102.

(24) Mori-Sánchez, P.; Cohen, A. J.; Yang, W. Localization and Delocalization Errors in Density Functional Theory and Implications for Band-Gap Prediction. *Phys. Rev. Lett.* **2008**, *100*, 146401.

(25) Cohen, A. J.; Mori-Sánchez, P.; Yang, W. Insights into Current Limitations of Density Functional Theory. *Science* **2008**, *321*, 792–794.

(26) Cohen, A. J.; Mori-Sánchez, P.; Yang, W. Fractional Spins and Static Correlation Error in Density Functional Theory. *J. Chem. Phys.* **2008**, *129*, 121104.

(27) Mori-Sánchez, P.; Cohen, A. J.; Yang, W. Discontinuous Nature of the Exchange-Correlation Functional in Strongly Correlated Systems. *Phys. Rev. Lett.* **2009**, *102*, 066403.

(28) Cohen, A. J.; Mori-Sánchez, P.; Yang, W. Challenges for Density Functional Theory. *Chem. Rev.* **2012**, *112*, 289–320.

(29) Ruzsinszky, A.; Perdew, J. P.; Csonka, G. I.; Vydrov, O. A.; Scuseria, G. E. Spurious Fractional Charge on Dissociated Atoms: Pervasive and Resilient Self-Interaction Error of Common Density Functionals. *J. Chem. Phys.* **2006**, *125*, 194112.

(30) Ruzsinszky, A.; Perdew, J. P.; Csonka, G. I.; Vydrov, O. A.; Scuseria, G. E. Density Functionals that are One- and Two- are not Always Many-Electron Self-Interaction-Free, as Shown for  $H_2^+$ ,  $He_2^+$ ,  $LiH^+$ , and  $Ne_2^+$ . *J. Chem. Phys.* **2007**, *126*, 104102.

(31) Vydrov, O. A.; Scuseria, G. E.; Perdew, J. P. Tests of Functionals for Systems with Fractional Electron Number. *J. Chem. Phys.* **2007**, *126*, 154109.

(32) Perdew, J. P.; Ruzsinszky, A.; Csonka, G. I.; Vydrov, O. A.; Scuseria, G. E.; Staroverov, V. N.; Tao, J. Exchange and Correlation in Open Systems of Fluctuating Electron Number. *Phys. Rev. A: At., Mol., Opt. Phys.* **2007**, *76*, 040501.

(33) Haunschmid, R.; Henderson, T. M.; Jiménez-Hoyos, C. A.; Scuseria, G. E. Many-Electron Self-Interaction and Spin Polarization Errors in Local Hybrid Density Functionals. *J. Chem. Phys.* **2010**, *133*, 134116.

(34) Perdew, J. P.; Parr, R. G.; Levy, M.; Balduz, J. L. Density-Functional Theory for Fractional Particle Number: Derivative Discontinuities of the Energy. *Phys. Rev. Lett.* **1982**, *49*, 1691–1694.

(35) Yang, W.; Zhang, Y.; Ayers, P. W. Degenerate Ground States and a Fractional Number of Electrons in Density and Reduced Density Matrix Functional Theory. *Phys. Rev. Lett.* **2000**, *84*, 5172–5175.

(36) Zhang, Y.; Yang, W. Perspective on “Density-Functional Theory for Fractional Particle Number: Derivative Discontinuities of the Energy. *Theor. Chem. Acc.* **2000**, *103*, 346–348.

(37) Zhao, Y.; Lynch, B. J.; Truhlar, D. G. Doubly Hybrid Meta DFT: New Multi-Coefficient Correlation and Density Functional Methods for Thermochemistry and Thermochemical Kinetics. *J. Phys. Chem. A* **2004**, *108*, 4786–4791.

(38) Grimme, S. Semiempirical Hybrid Density Functional with Perturbative Second-Order Correlation. *J. Chem. Phys.* **2006**, *124*, 034108.

(39) Zhang, Y.; Xu, X.; Goddard, W. A. Doubly Hybrid Density Functional for Accurate Descriptions of Nonbond Interactions, Thermochemistry, and Thermochemical Kinetics. *Proc. Natl. Acad. Sci. U. S. A.* **2009**, *106*, 4963–4968.

(40) Chai, J.-D.; Head-Gordon, M. Long-Range Corrected Double-Hybrid Density Functionals. *J. Chem. Phys.* **2009**, *131*, 174105.

(41) Su, N. Q.; Yang, W.; Mori-Sánchez, P.; Xu, X. Fractional Charge Behavior and Band Gap Predictions with the XYG3 Type of Doubly Hybrid Density Functionals. *J. Phys. Chem. A* **2014**, *118*, 9201–9211.

(42) Gill, P. M. W.; Adamson, R. D.; Pople, J. A. Coulomb-Attenuated Exchange Energy Density Functionals. *Mol. Phys.* **1996**, *88*, 1005–1009.

(43) Savin, A. In *Recent Developments and Applications of Modern Density Functional Theory*; Seminario, J. M., Ed.; Elsevier: Amsterdam, 1996; p 327.

(44) Leininger, T.; Stoll, H.; Werner, H. J.; Savin, A. Combining Long-Range Configuration Interaction with Short-Range Density Functionals. *Chem. Phys. Lett.* **1997**, *275*, 151–160.

(45) Iikura, H.; Tsuneda, T.; Yanai, T.; Hirao, K. A Long-Range Correction Scheme for Generalized-Gradient-Approximation Exchange Functionals. *J. Chem. Phys.* **2001**, *115*, 3540–3544.

(46) Baer, R.; Livshits, E.; Salzner, U. Tuned Range-Separated Hybrids in Density Functional Theory. *Annu. Rev. Phys. Chem.* **2010**, *61*, 85–109.

(47) Stein, T.; Eisenberg, H.; Kronik, L.; Baer, R. Fundamental Gaps in Finite Systems from Eigenvalues of a Generalized Kohn-Sham Method. *Phys. Rev. Lett.* **2010**, *105*, 266802.

(48) Tsuneda, T.; Song, J. W.; Suzuki, S.; Hirao, K. On Koopmans’ Theorem in Density Functional Theory. *J. Chem. Phys.* **2010**, *133*, 174101.

(49) Heyd, J.; Scuseria, G. E.; Ernzerhof, M. Hybrid Functionals Based on a Screened Coulomb Potential. *J. Chem. Phys.* **2003**, *118*, 8207.

(50) Yanai, T.; Tew, D. P.; Handy, N. C. A New Hybrid Exchange-Correlation Functional Using the Coulomb-Attenuating Method (CAM-B3LYP). *Chem. Phys. Lett.* **2004**, *393*, 51.

(51) Baer, R.; Neuhauser, D. Density Functional Theory with Correct Long-Range Asymptotic Behavior. *Phys. Rev. Lett.* **2005**, *94*, 043002.

(52) Cohen, A. J.; Mori-Sánchez, P.; Yang, W. Development of Exchange-Correlation Functionals with Minimal Many-Electron Self-Interaction Error. *J. Chem. Phys.* **2007**, *126*, 191109.

(53) Song, J. W.; Hirosawa, T.; Tsuneda, T.; Hirao, K. Long-Range Corrected Density Functional Calculations of Chemical Reactions: Redetermination of Parameter. *J. Chem. Phys.* **2007**, *126*, 154105.

(54) Chai, J. D.; Head-Gordon, M. Systematic Optimization of Long-Range Corrected Hybrid Density Functionals. *J. Chem. Phys.* **2008**, *128*, 084106.

(55) Li, C.; Zheng, X.; Su, N. Q.; Yang, W. Localized Orbital Scaling Correction for Systematic Elimination of Delocalization Error in Density Functional Approximations. *Nat. Sci. Rev.* **2018**, *5*, 203.

(56) Dunning, T. H. Gaussian Basis Sets for Use in Correlated Molecular Calculations. I. The Atoms Boron Through Neon and Hydrogen. *J. Chem. Phys.* **1989**, *90*, 1007–1023.

(57) Foster, J. M.; Boys, S. F. Canonical Configurational Interaction Procedure. *Rev. Mod. Phys.* **1960**, *32*, 300–302.

(58) Anisimov, V. I.; Zaanen, J.; Andersen, O. K. Band Theory and Mott Insulators: Hubbard U Instead of Stoner I. *Phys. Rev. B: Condens. Matter Mater. Phys.* **1991**, *44*, 943–954.

(59) Anisimov, V.; Izumov, Y. *Electronic Structure of Strongly Correlated Materials*; Springer Series in Solid-State Sciences; Springer: Berlin, 2010.

(60) Kulik, H. J. Perspective: Treating Electron Over-Delocalization with the DFT+U Method. *J. Chem. Phys.* **2015**, *142*, 240901.

(61) Anisimov, V. I.; Kozhevnikov, A. V. Transition State Method and Wannier Functions. *Phys. Rev. B: Condens. Matter Mater. Phys.* **2005**, *72*, 075125.

(62) Ma, J.; Wang, L.-W. Using Wannier Functions to Improve Solid Band Gap Predictions in Density Functional Theory. *Sci. Rep.* **2016**, *6*, 24924.

(63) Su, N. Q.; Li, C.; Yang, W. Describing Strong Correlation with Fractional-Spin Correction in Density Functional Theory. *Proc. Natl. Acad. Sci. U. S. A.* **2018**, *115*, 9678–9683.

(64) Jin, Y.; Zhang, D.; Chen, Z.; Su, N. Q.; Yang, W. Generalized Optimized Effective Potential for Orbital Functionals and Self-

Consistent Calculation of Random Phase Approximations. *J. Phys. Chem. Lett.* **2017**, *8*, 4746–4751.

(65) Zheng, X.; Cohen, A. J.; Mori-Sánchez, P.; Hu, X.; Yang, W. Improving Band Gap Prediction in Density Functional Theory from Molecules to Solids. *Phys. Rev. Lett.* **2011**, *107*, 026403.

(66) Gygi, F.; Fattebert, J.-L.; Schwegler, E. Computation of Maximally Localized Wannier Functions Using a Simultaneous Diagonalization Algorithm. *Comput. Phys. Commun.* **2003**, *155*, 1–6.

(67) Giustino, F.; Pasquarello, A. Mixed Wannier-Bloch Functions for Electrons and Phonons in Periodic Systems. *Phys. Rev. Lett.* **2006**, *96*, 216403.

(68) Dawes, R.; Carrington, T. Using Simultaneous Diagonalization and Trace Minimization to Make an Efficient and Simple Multi-dimensional Basis for Solving the Vibrational Schrödinger Equation. *J. Chem. Phys.* **2006**, *124*, 054102.

(69) Peverati, R.; Truhlar, D. G. Quest for a Universal Density Functional: the Accuracy of Density Functionals Across a Broad Spectrum of Databases in Chemistry and Physics. *Philos. Trans. R. Soc., A* **2014**, *372*, 20120476.

(70) Curtiss, L. A.; Raghavachari, K.; Redfern, P. C.; Pople, J. A. Assessment of Gaussian-2 and Density Functional Theories for the Computation of Enthalpies of Formation. *J. Chem. Phys.* **1997**, *106*, 1063–1079.

(71) Cížek, J. *Advances in Chemical Physics*; Hariharan, P. C., Ed.; Wiley Interscience: New York, 1969; Vol. 14, p 35.

(72) Purvis, G. D., III; Bartlett, R. J. A Full Coupled-Cluster Singles and Doubles Model - the Inclusion of Disconnected Triples. *J. Chem. Phys.* **1982**, *76*, 1910.

(73) Pople, J. A.; Head-Gordon, M.; Raghavachari, K. Quadratic Configuration Interaction - a General Technique for Determining Electron Correlation Energies. *J. Chem. Phys.* **1987**, *87*, 5968.

(74) Schmidt, W. Photoelectron Spectra of Polynuclear Aromatics. V. Correlations with Ultraviolet Absorption Spectra in the Catacondensed Series. *J. Chem. Phys.* **1977**, *66*, 828–845.

(75) Hendon, C. H.; Tiana, D.; Murray, A. T.; Carbery, D. R.; Walsh, A. Helical Frontier Orbitals of Conjugated Linear Molecules. *Chem. Sci.* **2013**, *4*, 4278–4284.